A New Band-Splitting Filter for Guided-Millimeter-Wave Transmission Systems

NOBUO SUZUKI

Abstract—**A new Michelson-interferometer (MI) hybrid having a miter angle is developed for use as a millimeter-wave band-splitting filter. The construction and operating principle of the filter are described. The design method and the experimental results are also presented.**

This filter has low branching loss, yet keeps very wide band characteristics. For the 40–120-GHz-frequency-range filter with 35° miter angle, the branching loss is 0.68–1.56 dB. This is about 40 percent lower than that of the conventional MI filter. The input VSWR is less than 1.29 and the guard bandwidth is less than 250 MHz.

This filter can be used for the 40–120-GHz guided-millimeter-wave transmission systems.

I. Introduction

AMONG various filters proposed for use in the guided-millimeter-wave transmission systems, the Michelson-interferometer (MI)-type filter has very wide band and low-loss characteristics. In addition, this filter can be directly connected to the TE_{01}-mode waveguide line, offering practical advantages for installation.

Marcatili and Bisbee have reported the possibility of using this filter as a band-splitting filter [1]. Iiguchi has presented its design theory [2]. Recently, the experiment on this filter was conducted by Suzuki in the 40–120-GHz range, confirming its very wide band and low-loss characteristics [3], [4].

We describe here a new band-splitting filter which can substantially reduce the branching loss, yet keep the very wide band characteristics. First, the formulas and graphs that facilitate the practical filter design are presented. Next, we discuss its application to the guided-millimeter-wave systems and describe an experiment on the filter.

II. Design Formula

Fig. 1 shows a possible implementation of a new band-splitting filter. As in the conventional MI-type filter, this filter is constructed from two hybrids, high-pass filters, and waveguide elbows. However, in contrast to the conventional one, the filter has miter hybrids and elbows whose angle between two guide axes (2θ) is different from 90° as shown in Fig. 1. In so doing, we get better performances as explained later.

Suppose a signal having wide frequency spectra is incident upon port W. Hybrid H_A yields two waves in the upper and lower guides, dependent on the reflection and transmission coefficients of the dielectric sheet of H_A. A

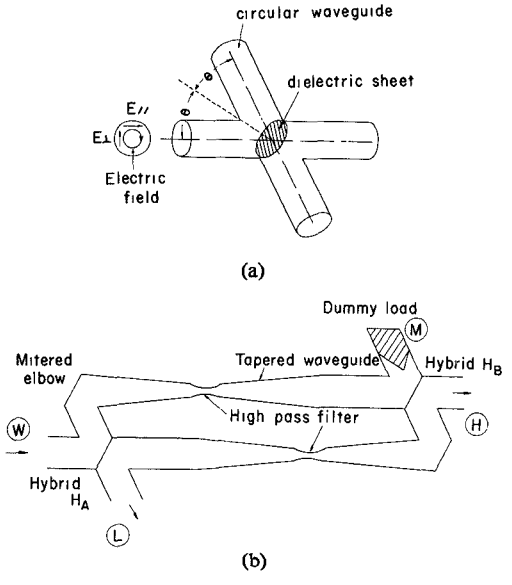

Fig. 1. Miter MI band-splitting filter. (a) Miter MI hybrid. (b) Fundamental construction.

part of these waves whose frequencies are below f_c is then reflected at the high-pass filters and emerges from ports L and W. The other part is transmitted through the high-pass filters, combined again by hybrid H_B, and emerges from ports H and M. The ideal band-splitting filter assumes, of course, that the signals emerge from ports L and H, but not from ports W and M.

Using the reflection and transmission coefficients R and D of H_A, the hybrid loss L_{B1} and the reflected power L_{R1} can be derived as follows [3]:

$$L_{B1} = -10 \log_{10} 4R^2D^2 \tag{1}$$

$$L_{R1} = 10 \log_{10} (R^2 - D^2)^2 \tag{2}$$

where mode conversion loss may be included in L_{B1}. Similarly, the hybrid loss L_{B2} and the residual coupling L_{R2} at ports H and M can be derived as follows:

$$L_{B2} = -10 \log_{10} (DR' + RD')^2 \tag{3}$$

$$L_{R2} = 10 \log_{10} (RR' - DD')^2 \tag{4}$$

where R' and D' are reflection and transmission coefficients of H_B, respectively, that are, in general, different from R and D of H_A.

As is well known, an isotropic dielectric sheet illuminated by obliquely incoming waves has different reflection and transmission coefficients with respect to the polarization of the waves. Hence, the TE_{01} mode transmitted through the dielectric sheet suffers mode conversions in accordance with

Manuscript received August 20, 1975; revised November 14, 1975.
The author is with the Millimeter-Wave Transmission Section, Trunk Transmission System Development Division, Yokosuka Electrical Communication Laboratory, Nippon Telegraph and Telephone Public Corporation, Yokosuka-shi, Kanagawa-ken 238-03, Japan.

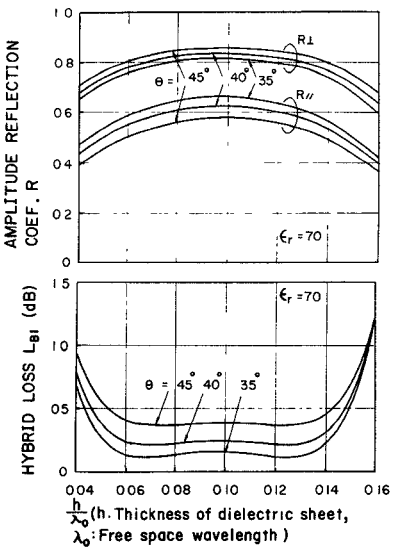

Fig. 2. Calculated amplitude reflection coefficient and hybrid loss versus h/λ_0.

the inclined angle of the sheet. This is apparent from the fact that the TE_{01} mode may be decomposed into two linearly polarized waves. The smaller we choose the inclined angle, the fewer mode conversions result. The filter presented here uses this characteristic to achieve better performances compared to the previous one [4].

The reflection and transmission coefficients are now written by

$$R = \tfrac{1}{2}(R_{\parallel} + R_{\perp}) \tag{5}$$

$$D = \tfrac{1}{2}(D_{\parallel} + D_{\perp}) \tag{6}$$

where

$$\left.\begin{aligned} R_{\perp} &= \left|\sqrt{r_{\perp}}\,\frac{1-A}{1-r_{\perp}\cdot A}\right| \\ D_{\perp} &= \left|d_{\perp}\,\frac{B}{1-r_{\perp}\cdot A}\right| \end{aligned}\right\} \tag{7}$$

$$\left.\begin{aligned} R_{\parallel} &= \left|\sqrt{r_{\parallel}}\,\frac{1-A}{1-r_{\parallel}\cdot A}\right| \\ D_{\parallel} &= \left|d_{\parallel}\,\frac{B}{1-r_{\parallel}\cdot A}\right| \end{aligned}\right\}, \tag{8}$$

$$A = \exp(-2j\delta), \qquad B = \exp(-j\delta)$$

$$2\delta = 2 \times \frac{2\pi h}{\lambda_0}\sqrt{\varepsilon_r - \sin^2\theta}$$

$$r_{\perp} = \frac{\varepsilon_r - \cos 2\theta(\varepsilon_r - 2\sin^2\theta) - 2\sin 2\theta \sin\theta\sqrt{\varepsilon_r - \sin^2\theta}}{\varepsilon_r - \cos 2\theta(\varepsilon_r - 2\sin^2\theta) + 2\sin 2\theta \sin\theta\sqrt{\varepsilon_r - \sin^2\theta}}$$

$$r_{\parallel} = r_{\perp} \times \frac{\varepsilon_r + \cos 2\theta(\varepsilon_r - 2\sin^2\theta) - 2\sin 2\theta \sin\theta\sqrt{\varepsilon_r - \sin^2\theta}}{\varepsilon_r + \cos 2\theta(\varepsilon_r - 2\sin^2\theta) + 2\sin 2\theta \sin\theta\sqrt{\varepsilon_r - \sin^2\theta}},$$

$$d_{\perp} = 1 - r_{\perp}, \qquad d_{\parallel} = 1 - r_{\parallel} \tag{9}$$

where h, ε_r, and λ_0 are sheet thickness, relative dielectric constant, and free-space wavelength, respectively. From the foregoing discussions, it is seen that $R^2 + D^2 < 1$ while $R_{\parallel}^2 + D_{\parallel}^2 = R_{\perp}^2 + D_{\perp}^2 = 1$. Simple calculation shows that the TE_{2n} and TM_{2n} modes are generated mainly at hybrids.

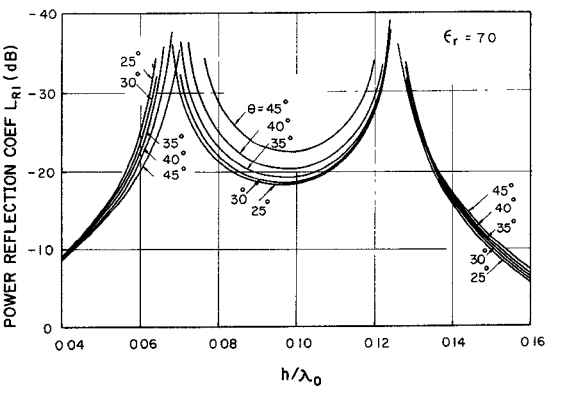

Fig. 3. Power reflection coefficient at port W with parameter θ.

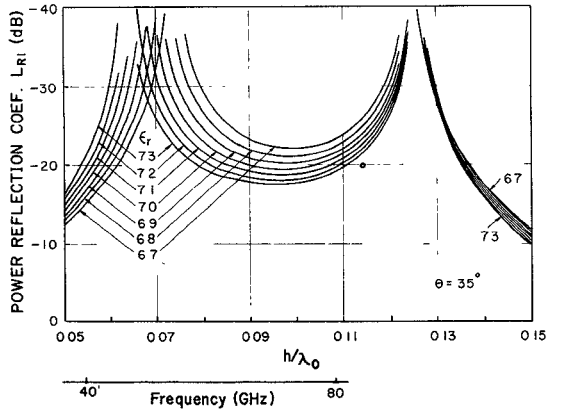

Fig. 4. Power reflection coefficient at port W with parameter ε_r.

We next present several design curves in Figs. 2–4. Fig. 2(a) shows R as a function of h/λ_0. The incident angle is varied from 35° to 45°, and the dielectric constant is assumed to be 7. Fig. 2(b) shows L_{B1} as a function of h/λ_0. If we choose the incident angle to be 35°, L_{B1} is 0.14 dB at 50 GHz, which is one-third that of the 45° hybrid. Figs. 3 and 4 show L_{R1} with parameters θ and ε_r, respectively. It is seen from Fig. 3 that the bandwidth increases with decreasing θ, and/or with increasing ε_r. Since the power reflection is usually required to be less than −18 dB, the 35° incident angle and dielectric constant of 7.1 is nearly optimum.

III. Application to the Guided-Millimeter-Wave System

A band-splitting filter used for the guided-millimeter-wave system is designed according to the following specifications: 1) frequency band, 40–120 GHz; 2) separation frequency, 80 GHz; 3) guard bandwidth,[1] below 300 MHz; 4) reflection

[1] The guard bandwidth is defined by the highest and lowest frequencies in port H and L of the band-splitting filter, respectively, where the signal level is attenuated to be −20 dB.

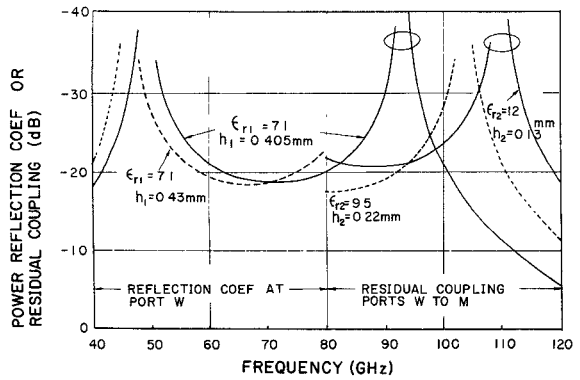

Fig. 5. Designed frequency response of 0-dB coupling characteristics.

coefficient, below −18 dB (VSWR: below 1.29); 5) residual coupling below −16 dB.

The separation frequency is almost coincident with the cutoff frequency f_c of the narrowest section of the cutoff filter, and thus the diameter of the section is chosen to be 4.571 mm. The guard bandwidth is mainly determined by the length and profile of the cutoff filter. For the design of the cutoff filter, see [5]. Dimensions of the cutoff filter are finally determined as follows: 1) taper waveguide section, cosine-cubed in shape, 150-mm length; 2) cutoff waveguide section, 4.571-mm ID, 16-mm length; 3) input and output waveguides, 10-mm ID.

The reflection characteristics of the filter are related to pulse echo resulting from multireflection. This specification is obtained from the allowable echo level of −29 dB of the multiplexing network.

Now, the coupling of hybrids H_A and H_B must be so chosen as to make the frequency response as flat as possible over the 40–120-GHz range. The wave in the lower band is not related to the hybrid H_B because it only round-trips in the hybrid H_A. Therefore, the hybrid H_A can be designed such that the coupling deviation in the 40–80-GHz band will be as small as possible. On the other hand, since the wave in the higher band goes through the hybrids H_A and H_B, the hybrid H_B is designed such that the overall coupling characteristics of the cascade connection of both hybrids is 0 dB.

First, we design the hybrid H_A. Fig. 4 shows that in the frequency band of 40–80 GHz the dielectric constant ε_r and the normalized thickness h/λ_0 are 7.1 and 0.054 (h = 0.405 mm at 40 GHz), respectively. These values satisfy a reflection coefficient below −18 dB. Fig. 5 shows the frequency response of this hybrid. The reflection level of port W is shown by the solid line.

Next, we design the hybrid H_B. The overall coupling must be as close as possible to 0 dB in the higher frequency band from 80 to 120 GHz. This is satisfied with the use of a different dielectric constant and thickness for H_B. Therefore, if

$$RR' - DD' = 0 \tag{10}$$

in the higher band of 80–120 GHz, the coupling loss of port W–H is 0 dB. The calculated value of (10) is shown in Fig. 6 with parameters ε_{r2} and h_2 for H_B, respectively. It is seen

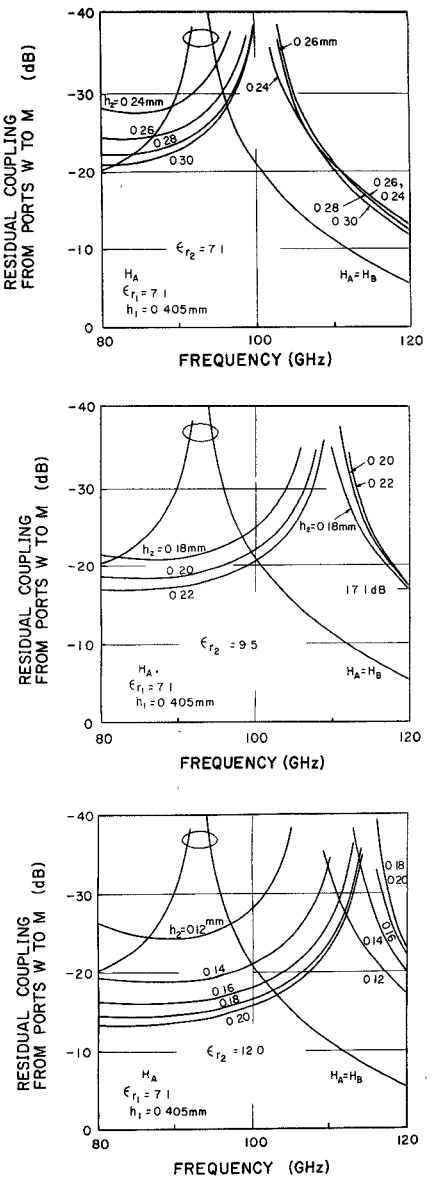

Fig. 6. Residual coupling in a higher frequency band with parameters ε_r and h. The curve indicated by $H_A = H_B$ means the frequency response where the hybrid H_B is the same as the hybrid H_A.

from Fig. 6 that the residual coupling decreases with increasing ε_{r2} or with decreasing h_2. Since we use 7.1 and 0.405 mm for ε_{r1} and h_1 of hybrid H_A, respectively, 12.0 and 0.13 mm may be optimum for ε_{r2} and h_2 of hybrid H_B, as shown in Fig. 5. This is satisfied with our specification of residual coupling value of −16.0 dB.

IV. Experimental Results

A. Hybrid

The manufacturing process for miter hybrids and elbow waveguides is as follows. First, cut diagonally in two the aluminum block of a rectangular prism. Next, sandwich a plane plate corresponding to a dielectric sheet between the aluminum blocks. Cylindrical holes of equal diameter (say 51 mm) are bored in such a way that the intersection of the axes of the waveguides makes angle of 35°.

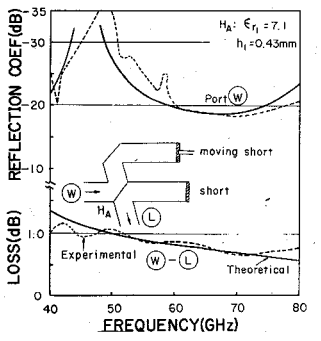

(a)

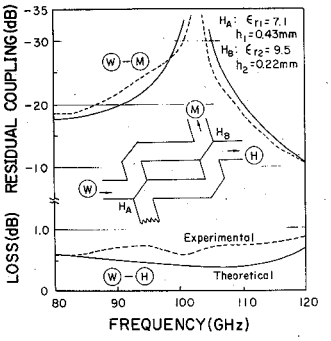

(b)

Fig. 7. Measured 0-dB coupling characteristics of lower and higher frequency band. (a) Lower frequency band. (b) Higher frequency band.

Fig. 7 shows the experimental results of 0-dB coupling characteristics which agree with calculated values. Experimental parameters are decided as follows.

	H_A	H_B
Incident angle of dielectric sheet	35°	35°
Waveguide diameter	51 mm	51 mm
Dielectric Sheet	Forsterite	Alumina
Dielectric constant	7.1	9.5
tan δ	$\sim 10^{-3}$	$\sim 10^{-4}$
Thickness	0.43 mm	0.22 mm

The thickness of the dielectric sheet for H_A is chosen to be longer than the previously calculated value in order to reduce the reflection coefficient near 40 GHz. Therefore, to avoid the increase of the residual coupling near 120 GHz, the parameters h_2 and ε_{r2} of the H_B must be decided optimally. However, we obtained h_2 and ε_{r2} of Fig. 7(b) because of the importance placed upon the characteristics near the separation frequency rather than 120 GHz related to the transmit–receive interference. As shown in Fig. 7(b), residual coupling deteriorates to be -11 dB near 120 GHz, and the coupling loss is increased by 0.36 dB.

The theoretical loss includes: 1) hybrid loss L_{B1} or L_{B2} (including coupling loss); 2) mode-conversion loss caused in a hybrid with miter circular waveguide; 3) tan δ loss; and 4) mode-conversion loss in an elbow waveguide. Here, 2) and 4) are treated in the same fashion to evaluate the loss in two elbows in the high- or low-frequency band.

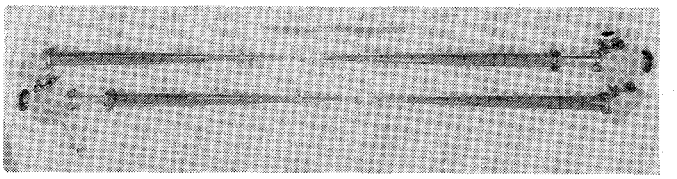

(a)

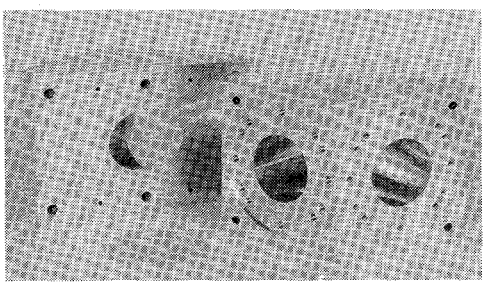

(b)

Fig. 8. 40–120-GHz filter. (a) Band-splitting filter. (b) Hybrid.

The loss in single elbow is given by [6]

$$L_e = -20 \log_{10} \left\{ 1 - 0.279 \left(\frac{\lambda_0}{a} \right)^{3/2} \right\} \qquad (11)$$

where a is the waveguide radius. Equation (11) has been derived for the right-angle elbow. The diffraction loss for the miter elbow used in this experiment would be larger than the loss given by (11). Hence, (11) should be understood to give a lower limit to the miter elbow diffraction loss. If, tan δ is less than 10^{-3}, the tan δ loss may be ignored because it is only 0.04 dB at 120 GHz.

B. Band-Splitting Filter

We have constructed a band-splitting filter as shown in Fig. 1(b). Fig. 8(a) shows a photograph of the complete band-splitting filter. The total length is 2.74 m.

The cutoff filter is made by electroforming, except for the taper waveguide section that uses a mandrel whose figure is step-wise shaped by a numerically controlled machine. The tapered waveguide from 51 mm to 10 mm in diameter is of the raised-cosine type [7], 1-m long, where the power level of the TE_{02} mode is below -40 dB.

Finally, the frequency response of the band-splitting filter is shown in Fig. 9 which was measured using a backward-wave-oscillator (BWO) sweep generator. As is shown in the figure, the loss in the lower frequency range is 0.80–1.56 dB, and the loss in the higher frequency range is 0.58–1.25 dB (0.68–0.85 dB in the 82–115-GHz range). The increase of the loss near 120 GHz is caused by degradation of the residual coupling characteristics. If we employ ideal parameters for the dielectric sheet in Fig. 5, the loss can be reduced.

The frequency interval at the 20-dB point of the losses W–H and W–L is 250 MHz, the deviation of f_c is $+25$ MHz, and the reflection level of the stopband is less than -20 dB. These values satisfy the specifications. The characteristics of VSWR of port W and residual coupling W–M are similar to the characteristics of Fig. 7. Thus VSWR of

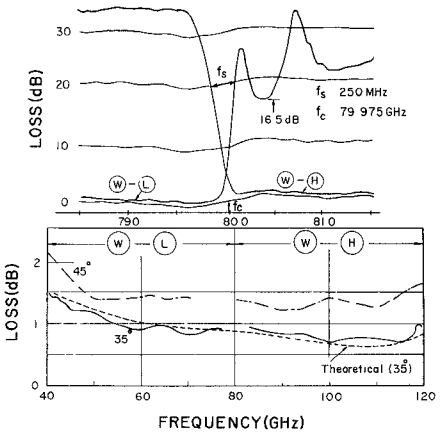

Fig. 9. Measured frequency response. The dot–dash line indicated by 45° is, for comparison, taken from [4].

port W is less than 1.22 (reflection loss -20 dB) over 40–58 GHz and less than 1.29 (reflection loss -18 dB) over 58–80 GHz. The characteristics of port L are similar to the characteristics of port W. The residual coupling is less than -16 dB over 80–110 GHz, and it is -11 dB at 120 GHz. VSWR of port H is 1.07 (reflection level -30 dB) in the higher frequency range.

V. Conclusions

The design and experiments of a new MI filter with 35° miter angle for guided-millimeter-wave transmission systems has been described.

This filter is constructed from two MI hybrids, high-pass filters, and waveguide elbows. Of particular interest are the hybrids having a miter angle because of their good performance. For example, if we choose a hybrid with 35° miter angle, the 0 dB coupling loss is 0.14 dB at 50 GHz, which is one-third of a conventional hybrid. And also, a super-wide band and low-loss bandsplitting filter with a loss of 0.68–1.56 dB in the frequency range 40–120 GHz has been realized. This is about 40 percent lower than the conventional MI-type filter. The VSWR is less than 1.29 in the lower frequency band and is less than 1.07 in the higher frequency band. The guard bandwidth is less than 250 MHz.

Though the total length for the experimental model is 2.74 m, if we employ an ideal design for the tapered waveguide, the length can be reduced by 35 percent.

This filter has 0.8-dB branching loss in the 100-GHz band, so it is particularly suitable for use at a much higher frequency.

Acknowledgment

The author wishes to thank Dr. M. Shimba and Dr. S. Shimada for their constant encouragement and M. Koyama and I. Ohtomo for their helpful comments. The author also wishes to thank K. Yoshida for his assistance in the experiments.

References

[1] E. A. Marcatili and D. L. Bisbee, "Band splitting filter," *Bell Syst. Tech. J.*, vol. 40, pp. 197–212, 1961.
[2] S. Iiguchi, "Michelson interferometer type hybrid for circular TE_{01} wave and its application to band splitting filter," *Rev. Elec. Commun. Lab.*, vol. 10, pp. 631–642, Nov.–Dec. 1962.
[3] N. Suzuki, "Millimeter-wave wideband Michelson-interferometer-type band-splitting filter," *Trans. Inst. Electron. Commun. Eng. Jap.*, vol. 56-B, pp. 51–58, 1973.
[4] ——, "A 40–120-GHz Michelson-interferometer-type band-splitting filter," *IEEE Trans. Microwave Theory Tech.* (Short Papers), vol. MTT-22, pp. 565–566, May 1974.
[5] N. Suzuki and S. Shimada, "Cosine-type cutoff filter for millimeter waves," *Trans. Inst. Electron. Commun. Eng. Jap.*, vol. 52-B, pp. 768–775, Dec. 1969.
[6] E. A. J. Marcatili, "Miter elbow for circular electric mode," in *Proc. Symp. Quasi-Optics.* New York: Polytechnic Press, 1964, pp. 535–543.
[7] H. G. Unger, "Circular waveguide taper of improved design," *Bell Syst. Tech. J.*, vol. 37, pp. 899–912, July 1958.